

STRUCTURE OF WOBBLING EXCITATIONS IN ^{163}Lu

B. GILLIS CARLSSON

*Division of Mathematical Physics, LTH, Lund University,
P.O. Box 118, SE-221 00 Lund, Sweden
gillis.carlsson@matfys.lth.se*

Received October 25, 2006

Using a many-particles plus rotor model, wobbling excitations built on top of a triaxial superdeformed band in ^{163}Lu are investigated. By extracting all parameters for the rotor from a mean field calculation a good correspondence with calculations based on the random-phase approximation is achieved.

1. Introduction

A type of excitation expected to occur in triaxial rotating nuclei is the so called wobbling excitation. The basic features of this excitation has been discussed on the basis of the asymmetric rotor model.¹ If the nucleus is originally rotating around the principal axis with largest moment of inertia, a wobbling excitation can be formed by tilting the total spin vector away from this axis. In the case of the asymmetric rotor the operator for this excitation can approximately be written as a boson operator carrying angular momentum away from this axis. Experimental evidence for this type of excitation has been seen in several odd-even Lu isotopes. Experimental data in ^{163}Lu (see e.g. Refs.^{2,3}) has been discussed using the one particle plus rotor model.⁴ A different approach based on the cranking + random-phase approximation (RPA) has also been used in order to describe the lowest observed wobbling band in this nucleus.^{5,6} However calculated $B(E2)$ ratios were smaller than experimental data by a factor of 2–3.

In this paper, a many particles plus rotor model (PRM) based on a triaxial core is used for the study of wobbling excitations in ^{163}Lu . This model was recently applied to describe states in ^{199}Pb with large K values and the role of the shears mechanism in the generation of angular momentum was discussed for different rotational bands.⁷

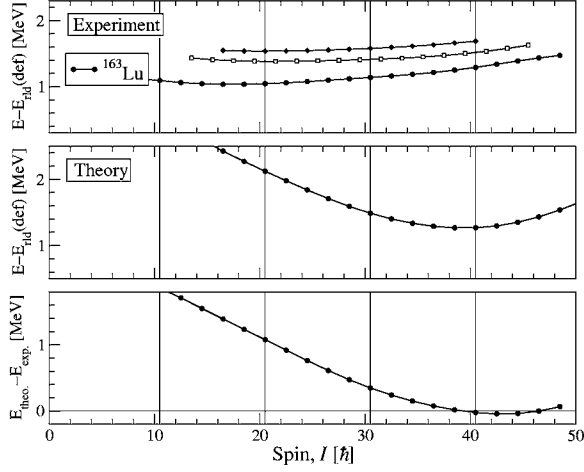


Fig. 1. Cranked Nilsson-Strutinsky (CNS) calculations for ^{163}Lu compared with experimental data.³ The upper panel shows the three experimental bands labeled TSD1, TSD2 and TSD3 relative to the energy of a rotating liquid drop. The calculated band is illustrated in the middle panel and the difference between experiment and theory is shown in the lower panel. The A150 parameters⁸ have been used and pairing is neglected. The deformation obtained at spin 30.5 is $\varepsilon_2 = 0.39$, $\gamma = 20^\circ$ and $\varepsilon_4 = 0.024$.

2. Cranked-Nilsson Strutinsky Calculations

In figure 1 the cranked Nilsson-Strutinsky (CNS)^{9,10,11} method is used to calculate the lowest triaxial superdeformed (TSD) band in ^{163}Lu . The experimental data show two more bands that have been interpreted as wobbling excitations. The CNS calculations are carried out by minimizing the energy with respect to deformation but without any pairing interaction included. Based on these calculations, the most likely configuration for the yrast triaxial superdeformed (TSD) band is $\pi(i_{13/2})^1(h_{11/2})^{-4}(f_{7/2}h_{9/2})^2(N=4)^{-10}$ for the protons and $\nu(i_{13/2})^6(h_{11/2})^{-2}(f_{7/2}h_{9/2})^8(N=4)^{-2}$ for the neutrons. When using calculations with pairing but without particle-number projection the pairing deltas become zero at $\hbar\omega = 0.4$ MeV¹² which corresponds roughly to spin 30.5. The deformation dependence has been investigated using cranked Nilsson-Strutinsky calculations with pairing and the deformation was found to vary only slightly as a function of spin ($\varepsilon_2 \simeq 0.38 - 0.41$ and $\gamma \simeq 19.5^\circ - 21.5^\circ$).²

In the following, in order to keep the PRM calculations simple, zero pairing is assumed also in these calculations along with a constant deformation of ($\varepsilon_2 = 0.4, \gamma = 20^\circ$) in the Lund convention. With a particle space built from the $i_{13/2}$ proton and the six $i_{13/2}$ neutrons, a large part of the total spin can be treated microscopically. This choice means that at spin 20.5, roughly 50 % of the total spin comes from these particles and at spin 40.5, about 40 % of the total spin.

3. Model

The model used is based on single-particle orbitals in a deformed potential in a similar way as the two-quasiparticle plus rotor model of Ref.¹³ Compared with Ref.¹³, it is formulated for an arbitrary number of (quasi-)particles but with the drawback that pairing is neglected at present. The Hamiltonian can be written (cf. Refs.^{1,13,14})

$$H = H_{rot} + h_{s.p.} = \sum_{k=1}^3 \frac{R_k^2}{2\mathcal{J}_k} + h_{s.p.} = \sum_{k=1}^3 \frac{(I_k - j_k)^2}{2\mathcal{J}_k} + h_{s.p.} \quad (1)$$

with $h_{s.p.} = \sum_i e_i a_i^\dagger a_i$. Here the e_i 's are the single-particle energies of the deformed modified oscillator. The strong coupling basis functions,¹⁵

$$\begin{aligned} |\Psi_{MK\alpha}^I\rangle &= \frac{N_{\alpha K}}{\sqrt{2}} (1 + e^{-ij_2\pi} e^{iI_2\pi}) |IMK\rangle |\alpha\rangle \\ &= \frac{N_{\alpha K}}{\sqrt{2}} (|IMK\rangle |\alpha\rangle + (-1)^{I-K} |IM-K\rangle |\tilde{\alpha}\rangle), \end{aligned} \quad (2)$$

have the normalization constant $N_{\alpha K}$ equal to one except when $K = 0$ and the rotated state $|\tilde{\alpha}\rangle = e^{-ij_2\pi} |\alpha\rangle$ is the same as $|\alpha\rangle$ which happens when an even number of particles are placed in time-reversed orbits. In this case a different normalization is required, $N_{\alpha K} = \frac{1}{\sqrt{2}}$. Slater determinants are used for the particle states $|\alpha\rangle = \left(\prod_{i=1}^{N_p} a_{\beta_i}^\dagger\right) \left(\prod_{i=1}^{N_n} a_{\gamma_i}^\dagger\right) |0\rangle$ where the number of protons (neutrons) treated explicitly is denoted by N_p (N_n).

The PRM Hamiltonian (Eq. (1)) gives rise to both one-particle one-hole and also two-particle two-hole couplings between the basis states. The general procedure for solving the Hamiltonian consists of defining a part of the single-particle space as belonging to the core and a part belonging to the particles. When considering a few particles in a high- j shell such as an $i_{13/2}$ shell, the couplings to other states outside this shell are generally small since the nearby levels often have a different parity.

After diagonalization, wavefunctions with good total spin I are obtained from which transition strengths can be calculated. The core properties that has to be known are the three moments of inertia and also the gyromagnetic factor g_R when calculating $B(M1)$ values and quadrupole moments $Q_{2\mu}$ for $B(E2)$ values.

In order to illustrate the structure of the wavefunctions one can calculate the projection of the total spin on different axes. Choosing the 1-axis as an example, states with $I_1 = \Omega$ are projected out using the operator:¹⁶

$$P^\Omega = \int_0^{2\pi} e^{i\phi(I_1-\Omega)} \delta\phi. \quad (3)$$

The basis states are eigenstates of I_3 which can be used when calculating projections on other axes. Taking the I_1 operator as an example, the transformation

$$e^{i\phi(I_1-\Omega)} = e^{i\phi(e^{iI_2\pi/2} I_3 e^{-iI_2\pi/2} - \Omega)} = e^{iI_2\pi/2} e^{i\phi(I_3-\Omega)} e^{-iI_2\pi/2} \quad (4)$$

is useful. When deriving this relation one has to keep in mind that the angular momentum operators are defined in the body-fixed frame so their commutation

relations are given as $[I_1, I_2] = -iI_3$ and cyclic permutations. For an $|IMK\rangle$ state, the projection amounts to

$$\begin{aligned} & \langle IMK' | P^\Omega | IMK \rangle \\ &= \frac{1}{2\pi} \int_0^{2\pi} \sum_{l,l'} \langle IMK' | e^{iI_2\pi/2} | IMl \rangle \langle IMl | e^{i\phi(I_3-\Omega)} | IMl' \rangle \langle IMl' | e^{-iI_2\pi/2} | IMK \rangle \delta\phi \\ &= d_{K'\Omega}^I(-\pi/2) d_{K\Omega}^I(-\pi/2). \end{aligned} \quad (5)$$

In the derivation above the fact that the matrix elements of I_2 have opposite sign compared to the ones of I_y in the laboratory frame has been used when making the identification with the $d_{K'\Omega}^I$ functions. Between two of the basis states (Eq. (2)) the result becomes

$$\begin{aligned} W_\Omega &= \langle \Psi' | P^\Omega | \Psi \rangle = \frac{1}{2\pi} \int_0^{2\pi} \langle \Psi' | e^{i\phi(I_1-\Omega)} | \Psi \rangle \delta\phi \\ &= \frac{N_{\alpha K} N_{\alpha' K'}}{2} (d_{K'\Omega}^I(-\pi/2) d_{K\Omega}^I(-\pi/2) + d_{-K'\Omega}^I(-\pi/2) d_{-K\Omega}^I(-\pi/2)) \langle \alpha' | \alpha \rangle \\ &+ (-1)^{I-K} \frac{N_{\alpha K} N_{\alpha' K'}}{2} (d_{K'\Omega}^I(-\pi/2) d_{-K\Omega}^I(-\pi/2) + d_{-K'\Omega}^I(-\pi/2) d_{K\Omega}^I(-\pi/2)) \\ &\times \langle \alpha' | \tilde{\alpha} \rangle. \end{aligned} \quad (6)$$

Similar formulas are obtained for the I_2 axis while the I_3 axis is simpler since there is no need to rotate the projection operator. The $d_{K'\Omega}^I$ functions are calculated numerically using the recursive iteration described in Ref.¹⁷

3.1. Rotor parameters

In order to describe the rotation of a triaxial nucleus in the PRM, one needs three moments of inertia. In the present contribution they are obtained from CNS calcu-

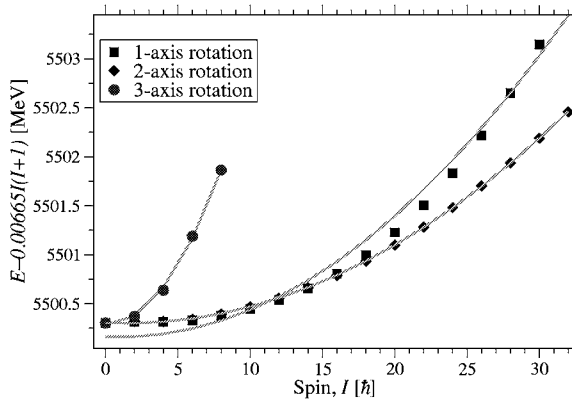


Fig. 2. (Color online) Total energy minus a rigid rotor reference for rotation of the core around the three different principal axes in ^{163}Lu . The points are obtained from CNS calculations without Strutinsky corrections and the lines show the result of fitting functions of the form $E_0 + \frac{I^2}{2\mathcal{J}}$ to the points. The values of \mathcal{J} obtained from these fits are used as moments of inertias for the rotor.

lations without Strutinsky corrections. The total energy of the core as a function of core spin for rotation in three different directions is illustrated in figure 2. The nucleus built from core + particles prefers to rotate along the 1-axis although for the core, rotation around the 2-axis is energetically more favorable. From this figure three moments of inertia can be extracted which are used for the rotor. The quadrupole moments for the core are calculated from the cranking wavefunction as a function of rotor spin (for rotation in the 1-direction) and average values (not very different from the values at spin 0) are used when calculating the $B(E2)$ values.

4. Results for ^{163}Lu

As mentioned one $i_{13/2}$ proton and six $i_{13/2}$ neutrons are included in the particle space. The 14 energy levels belonging to the deformed $i_{13/2}$ shells for protons and neutrons, respectively, are used as basis states for these particles. A many-particle basis of Slater determinants is then constructed by taking all possible particle-hole excitations within this space. In this case one obtains a total of 21021 basis states of each signature. Each basis state can be combined with different K values. The difference between the K value and the expectation value of $\langle j_3 \rangle$ for each Slater determinant is a measure of how much spin in the 3-direction is borrowed from the rotor. In order to reduce the size of the matrices which have to be diagonalized a truncation in this quantity is employed. The results appear to be converged if this difference is allowed to be 10 units which gives 210243 basis states for each signature. Diagonalization is then performed separately for each spin using Lancos method.¹⁸

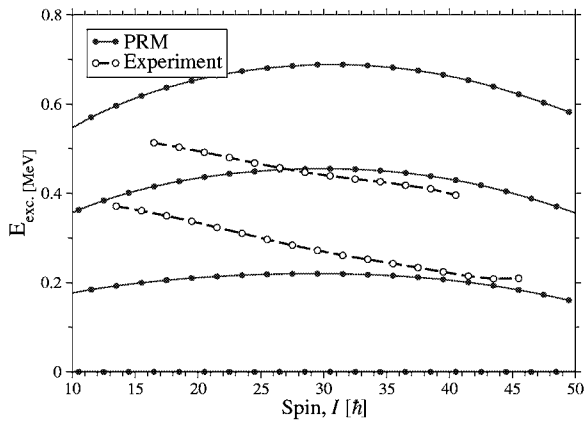


Fig. 3. (Color online) Wobbling excitation energy for ^{163}Lu . The lowest band having even+1/2 spins is interpolated to obtain energies for odd+1/2 spins. This energy is then subtracted from the energy of the lowest three excited bands. The same procedure is used both for experimental³ and calculated states.

The calculated wobbling excitation energy is illustrated in figure 3. As seen from this figure there is a reasonable agreement with experimental data in the high-spin region. The wobbling excitation energy was previously calculated in the random-phase approximation (RPA) using a fixed deformation of ($\varepsilon_2 = 0.43, \gamma = 20^\circ$) and small pairing delta's ($\Delta_p = \Delta_n = 0.3$).⁵ Although the comparison in Ref.⁵ is made as a function of cranking frequency the results for the lowest wobbling excitation energy are very similar to the ones in figure 3.

Since the core prefers to rotate along the 2-axis, the system as a whole will switch rotational axis at high spin. If this transition goes smoothly it may be associated with a region of tilted axis rotation where the yrast band and the first wobbling band becomes degenerate. It appears likely that the decrease of the excitation energy seen at high spin indicates the onset of such a transition.

The calculated energy difference between the bands is rather constant as expected from the analysis using the asymmetric rotor model.¹ Thus the explicit inclusion of the six $i_{13/2}$ neutrons does not help to explain the anharmonicity in the excitation energy seen at lower spin. However in this region pairing is certainly important and should be included for a better description.

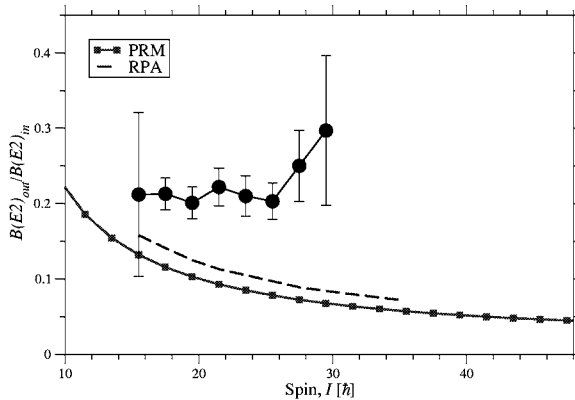


Fig. 4. (Color online) Reduced transition probabilities for the transitions from the first wobbling band to the lowest band divided by the same quantity for the transitions within the wobbling band. The data and calculations are shown as a function of the spin of the initial state. The experimental data are obtained from Refs.^{2,3,19} and the result of the RPA calculations is taken from Ref.⁶.

Figure 4 shows the ratio of $B(E2)$ transition strengths between the first wobbling band and the lowest TSD band and the intra-band transitions. The PRM calculations without any pairing may not be expected to give an accurate description of the transitions below roughly spin 30. However it is interesting to note that the RPA calculations with small pairing delta's give roughly the same result as the PRM. In Ref.⁶ it was shown that changing the triaxiality parameter γ to 30° improves the agreement with experiment but as also concluded such a change can not be justi-

fied considering that minimizing with respect to deformation in Nilsson-Strutinsky calculations gives $\gamma \simeq 20^\circ$.²

Figures 5,6 and 7 shows the result of projecting out states with good spin projections from the total wavefunction. Eq.(6) is used along with similar equations for the other axes. As seen in Fig. 5 the lowest TSD band has a large spin component with $I_1 = I$ in the 1-direction. For the first excited band (Fig. 6), the largest component in the 1-direction is $I_1 = I - 1$ and the spin projections along the 2 axis increase a lot. The second excited band shown in Fig. 7 has a more complicated structure with an increasing number of nodes in the 2 direction. The largest spin component in the 1-direction has $I_1 = I$ but there are several components with smaller I_1 projections.

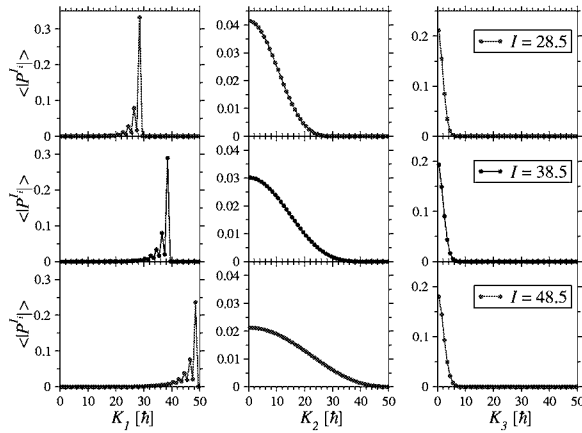


Fig. 5. (Color online) The probability of finding different spin projections in the wavefunction. Since the distributions are symmetric with respect to positive and negative projections only the positive ones are shown. The figure is constructed using the calculated wavefunctions for the lowest TSD band in ^{163}Lu .

5. Summary

Calculations for the TSD bands in ^{163}Lu are performed using a PRM model with seven particles and rotor parameters extracted from cranking calculations. The results appear to be similar to those of previous RPA calculations for the same states which for example means that the $B(E2)$ ratios are underestimated by roughly a factor of 2-3 compared with experiment. The structure of the excited bands is illustrated by projecting out components with good spin projections on various axes.

Acknowledgments

The author would like to thank Ingemar Ragnarsson for valuable discussions. This work was supported by the Swedish Science Research Council.

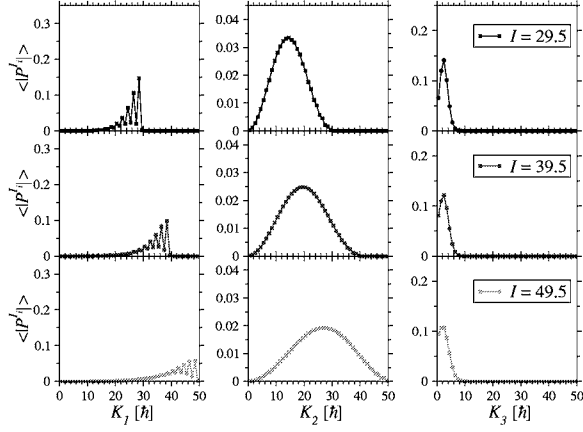


Fig. 6. (Color online) Similar to figure 5 but for the first excited TSD band in ^{163}Lu .

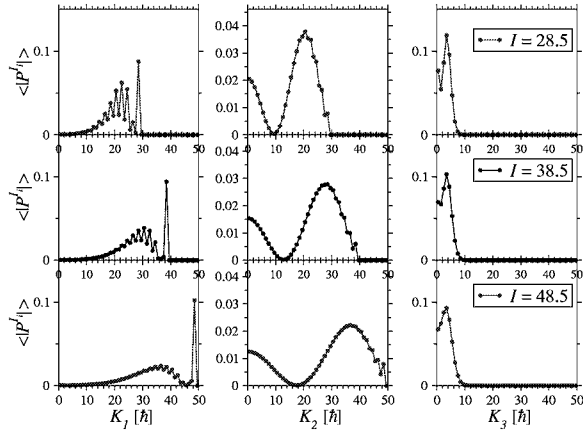


Fig. 7. (Color online) Similar to figure 5 but for the second excited TSD band in ^{163}Lu .

References

1. A. Bohr and B.R. Mottelson *Nuclear Structure vol. II* (W.A. Benjamin Inc, New York 1975).
2. A. Grgeren *et. al.*, Phys. Rev. C **69**, 031301(R) (2004).
3. D.R. Jensen *et. al.*, Nucl. Phys. **A703** 3 (2002).
4. I. Hamamoto and G. B. Hageman, Phys. Rev. C **67**, 014319 (2003).
5. M. Matsuzaki, Y. R. Shimizu and K. Matsuyanagi, Phys. Rev. C **65**, 041303(R) (2002).
6. Y. R. Shimizu, M. Matsuzaki and K. Matsuyanagi, Phys. Scr. **T125** 134 (2006).
7. B. G. Carlsson and Ingemar Ragnarsson Phys. Rev. C **74**, 044310 (2006).
8. The parameters usually referred to as A150 are the ones given in T. Bengtsson, Nucl. Phys. A512 (1990) 124, with the addition that μ has been changed from 0.69 to 0.60 for the proton $N = 6, 7$ shells.
9. T. Bengtsson and I. Ragnarsson, Nucl. Phys. **A436**, 14 (1985).

10. B.G. Carlsson and I. Ragnarsson, Phys. Rev. C **74**, 011302(R) (2006).
11. A.V. Afanasjev, D.B. Fossan, G.J. Lane and I. Ragnarsson, Phys. Rep. **322**, 1 (1999).
12. D. Almhed, R. G. Nazmitdinov and F. Döna, Phys. Scr. **T125** 139 (2006).
13. I. Ragnarsson and P.B. Semmes, Hyp. Int. **43**, 425 (1988).
14. S.E. Larsson, G. Leander and I. Ragnarsson, Nucl. Phys. **A307** 189 (1978).
15. D. J. Rowe, *Nuclear collective motion* (Butler and Tanner Ltd, Frome and London, 1970).
16. P. Ring and P. Schuck, *The Nuclear Many-body Problem*, Springer-Verlag, New York, 1980.
17. T. Risbo, Journal of Geodesy **70** 383 (1996).
18. ARPACK <http://www.caam.rice.edu/software/ARPACK/>
19. G. B. Hagemann, private communications